Deep-Sea Research I 57 (2010) 909–917

Contents lists available at ScienceDirect

Deep-Sea Research I

journal homepage: www.elsevier.com/locate/dsri

Instruments and Methods

Rapid swing and spin of [deep] taut-wire-moored instruments

Hans van Haren

Royal Netherlands Institute for Sea Research (NIOZ), PO Box 59, 1790 AB Den Burg, The Netherlands

ARTICLE INFO

Article history:
Received 9 October 2009
Received in revised form
1 February 2010
Accepted 21 April 2010
Available online 15 May 2010

Keywords:
Acoustic current meters
Taut-wire mooring
No flow-directing vane
Fast rotation

ABSTRACT

Rapid 'swing', compass variations O(10°) in O(10 s), and 'spin', complete rotations around the vertical axis within a few minutes, are a concern of acoustic current meters moored in-line. Observations are used from fast sampling, at once per 1 and 30 s, instrumentation on deep-ocean moorings mainly outside surface wave and bottom boundary influences. Such instruments do not require a vane common to some historic mechanical current meters and they are often moored in a much easier to handle sub-surface buoy or mounting rack, without vanes. In their mountings they are nearly symmetric, so that they can spin freely in (turbulent; shear) flows. A comparison is made between noise levels of such free spinning instrumentation with those of instruments mounted in a fixed bottom-frame and with those of instruments equipped with a vane to one side. Typical spinning has a single rotation varying between 40 and 200 s. Spinning is shown to be highly binary: on or off. Its effects are found negligible on estimates of ocean currents, provided compass updates are adequate as in existing instrumentation. Acoustic noise is O(10) times larger than noise due to spinning. Some effects of spinning are noticed in the acoustic echo amplitude showing higher noise at frequencies >100 cpd, cycles per day. The character of this noise changes dramatically due to spinning. However, it is mainly in the ocean turbulence range and does not affect measurements of internal waves or periodic zooplankton motions.

1. Introduction

Most traditional mechanical current meters consist of a vane, a compass and an impellor or rotor. As such an instrument needs to be directed into the flow, it has to be suspended freely in a mooring cable and balanced well horizontally. This partially mechanical device has its shortcomings, because of the minimum speed needed to overcome friction in the bearings of the rotor and because of the relatively slow response of the vane in turbulent waters (e.g., Pollard, 1973; Saunders, 1980; von Zweck and Saunders, 1981; Sherwin, 1988; Loder and Hamilton, 1991). These authors have suggested various corrections for such non-linear response under misalignment of the rotor in the flow due to surface wave action or mooring vibrations, for example. Harder to grasp are potential errors due to misreading of a compass when instruments are swinging fast, such as under surface waves and in turbulence, where typical swings of vaned instruments are across angles O(10°) in the horizontal plane. To its advantage, the effect of such irregular rotor misalignment in the flow is used to 'detect' qualitatively turbulent motions in boundary flows by means of relatively fast sampling, once per 60 s, conventional current meters (Hosegood and van Haren, 2003).

Such errors in current speed and direction inherent to mechanical current meters seemed obsolete with the advent of acoustic Doppler current meters. After all, the latter instrumentation does not rely on mechanical components, but on particles in the water. When sufficient particles are present, they can measure any current speed starting from zero to within the resolution of the instrument. As they do not need to be directed into the flow (because they are omni-directional) they are commonly clamped to a cable, or mounted with swivels in-line held in a frame or a buoy. The advantage of such construction without a vane is much easier handling during overboard operations. Some manufacturers of acoustic current meters still offer an asymmetric configuration option with a vane for flow orienting.

As acoustic current meters also use compasses, besides tilt sensors, to find the orientation of their acoustic beams in a fixed Cartesian frame of reference they are prone to compass reading errors, for example when they spin quickly. Such spinning or swinging is inherent to nearly symmetric objects freely suspended in a turbulent shear flow, such as buoys or current meters without a vane. When the true rotation is faster than the compass update rate, the compass may cause the assignment of erroneous orientation of the acoustic beams at given moments. Its effects on current measurements are studied here.

We will not consider mooring 'vibrations', a transverse sloshing back and forth of the instrument or mooring line, e.g., due to turbulence in the wake of a current passing moored

E-mail address: hans.van.haren@nioz.nl

0967-0637/$ - see front matter © 2010 Elsevier Ltd. All rights reserved.
doi:10.1016/j.dsr.2010.04.007

objects. Such 'Strouhal' vortex-shedding-induced vibrations have periods varying between 0.1 and 1 s and amplitudes O(10^{-2}–10^{-1} m) under typical ocean flow conditions (e.g., Loder and Hamilton, 1991). We will also not consider mooring 'deflections' associated with the main ocean flow obstruction under drag. These deflections are slow mooring motions like the ocean currents. The instrumentation under investigation has been designed to resolve these well, e.g., with O(100) times faster compass updates. Instead, we are interested in the effects of rotational swings in the horizontal plane that are slower than vibrations, but faster than deflections.

We distinguish an instrument 'swing' for compass variations O(10°) and periods O(10 s) from 'spins' for compass variations O(100°) and periods O(100 s). Such spins and swings are caused by the mean turbulent shear flow, whereby transversal energy is transferred to rotations via a torque (e.g., Bagchi and Balachandar, 2002), either building up tension in a cable without swivels or causing oscillations after relaxation of the swivels. Small torques are needed to cause rotation of nearly symmetrical objects, and once rotating there is little obstruction to halt it. In the present instrumentation set-up, cables are twisted steel, which are not specifically torque-balanced, but the swivels connecting them and instruments easily rotate freely under typical 4000 N tensions.

We investigate measurements from several types of acoustic current meters, including acoustic Doppler current profiler ADCP, in different mountings and in comparison with a mechanical, vaned current meter. Although such a vane will still induce some horizontal swing of an instrument, typically a few degrees, it is assumed to be relatively still compared to swivelled, more or less symmetric instruments. Except for one, a bottom-fixed frame, all moorings are long deep-ocean sub-surface taut-wire moorings from abyssal plains. On these long moorings, instrumentation and mooring elements are all far outside the influence of severe turbulent zones induced by surface wave or internal wave breaking, whilst the near-bottom end, the acoustic releases, may be under influence of bottom friction.

2. Data and background

For studies on deep-ocean internal waves we use taut-wire moorings that consist of a few km long, segmented, line of nylon coated 0.0055 m diameter twisted steel and topped with elliptical buoys of several 1000's N buoyancy (Fig. 1). The top-buoy is at least 500 m, more often 1000–1500 m below the surface. Typical tension in the cable amounts 4000 ± 1500 N and no additional buoyancy is used further down the line, except for a single extra buoy near the top when the line is heavily instrumented. This floatation set-up is to avoid entanglement of cable and instruments during retrieval, but has the disadvantage that if the top-buoy is lost, the entire mooring will be lost. So far this happened only once, after implosion of a current meter. All other 30+ retrievals went very smooth, recovering 4 km long instrumented lines within 2 h.

These deep-ocean moorings are designed for minimal drag. Under the current regimes of investigation, with speeds up to 0.25 m s^{-1}, the pressure sensor in the top-buoy shows their quality: the stretching of the cable, of about 0.001, is clearly visible during the first months of the record (Fig. 1c). Throughout the 1.5 years of moored period tidal motions are discernible in their spring-neap cycle, which are partially reflecting the hydrostatic surface pressure. The asymmetric part of spring-neap cycles shows the mooring deflection due to variable large-scale ocean currents. The top of the mooring never varies vertically by more than a few meters. The associated horizontal deflection of the top-buoy is O(100 m).

Instrumentation is connected between the mooring line segments via shackles and heavy-duty NIOZ swivels. These custom-made swivels have ceramic bearings and still rotate under tensions of up to 40 kN. These allow mounting of any instrument frame or buoy that is not a freely rotating, vaned mechanical current meter. Presently, less than 10% of NIOZ current meters are of this conventional type. The majority are several types of acoustic current meters or ADCPs of which all, except one, are used in a standard, easy-mountable rack-frame without vane (Table 1 for instrument characteristics). This makes most instrumentation more or less symmetric objects above or below swivels in a mooring line. Likewise, the ADCPs can also be mounted in an elliptical buoy, either in-line or as a top-buoy, both without vane making this construction also symmetric. The thin mooring line poses no acoustic contamination of data from the standard 75 kHz ADCP, confirming earlier findings by Schott (1988) also for clear, deep-ocean waters.

For studying internal waves interacting with sloping bottoms a thermistor string is mounted below a current meter and a 2000 N top-buoy and attached to a bottom lander frame. The frame holds a current meter and a 300 kHz ADCP that are thus both fixed in space in contrast with the in-line current meter. Contrary to the 75 kHz ADCP above, this 300 kHz ADCP regularly shows 'bad' data not exceeding the error threshold due to its lesser power and due to reflections at thermistors in waters of few scattering materials.

On 'short-term' moorings, which are left unattended for periods between one and three weeks for detailed process studies, instrumentation samples relatively fast, at rates between 0.03 and 1 Hz. Such rates are just about adequate to monitor mooring spin, in the best cases even mooring swing, but they are generally too slow to monitor Strouhal vibrations. On 'long-term' moorings, which are left unattended for 1.5 years to study climatologic variations, instrumentation typically samples once per 900 s. At such a rate we can only infer the effects of fast mooring motions by comparing data from different instruments, differently mounted. However, Nortek's AquaDopp acoustic current meter has the option of burst sampling in 'diagnostic mode'. In this experiment 30 samples are stored at a rate of 1 Hz every 24 h. Table 2 lists mooring characteristics of instrumentation described in this paper.

3. Compass functioning

One of the crucial parts in current meters is the compass and its correct functioning. Most magnetic, Hall-effect or flux-gate compasses cannot be tilted more than 20–30° from the horizontal for proper functioning. Therefore, most modern current meters are instrumented with a tilt sensor. The present mooring design specifically aims at correct upright positioning. Tilt typically amounts less than a few degrees, seldom exceeding $|10°|$.

In the case of potentially current error-inducing instrument-spin or -swing, it is imperative to know how the compass' update (response) relates to the rotation speed. For some instruments, like Aquadopp, compass update rates can be user-programmed, differently from acoustic pings if necessary. Others have fixed update periods, commonly larger than the times between acoustic pings. ADCPs update every acoustic ping. For a 75 kHz ADCP covering a range of 600 m, the compass will be updated about every 1 s. Typical compass updates vary between 1 and 10 s (Table 1). It is noted that the compass response rate need not be the same as the programmed update rate. Especially flux-gate compasses are expected to rapidly adjust themselves, so that a given reading is proper. This is assumed in the following test, in which we consider two hypothetical cases of rotating compasses

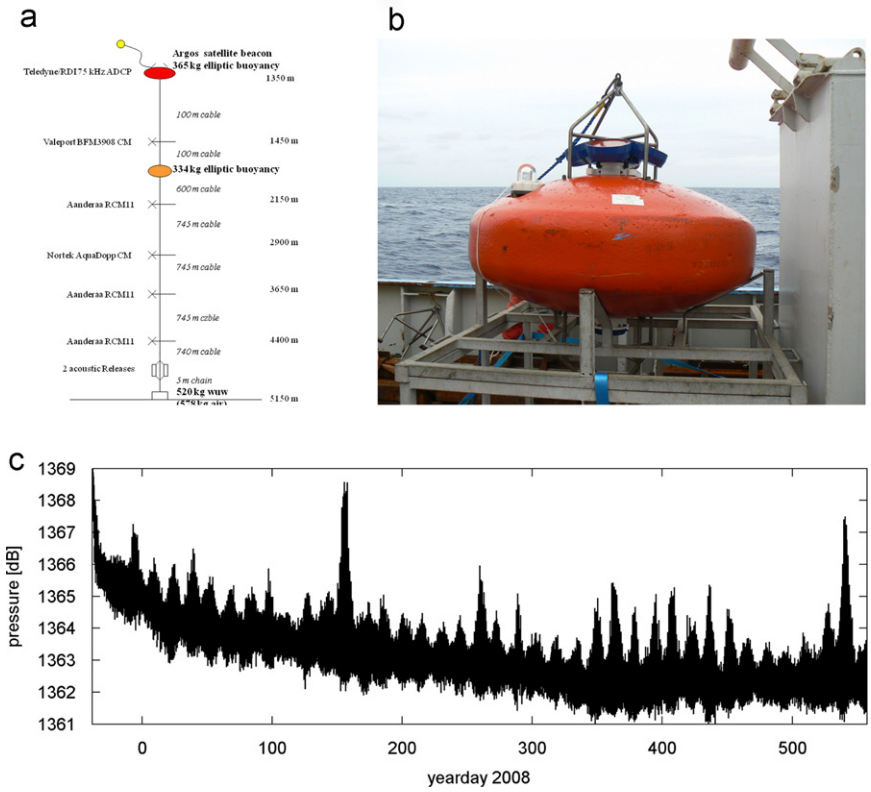

Fig. 1. (a) Typical mooring scheme of large, minimal drag ocean mooring LOCO11/4. (b) Top-buoy ADCP mounting (with satellite beacon). (c) Time series of 1.5 years pressure measured at the top-buoy of (a). Time is in yeardays 2008. Days in 2007 are −365 days, in 2009 +365 days.

Table 1
Different current meters CM and nominal noise levels/accuracy as provided by manufacturers. Typical compass updates are given for typical sampling rates. Acoustic instruments use fast-response flux-gate compasses, except for RCM11 that have Hall-effect magnetic compass.

Instrument name	Sampling int. (s)	Compass upd. (s)	Accuracy ($m\,s^{-1}$)	Mounting
Valeport BFM-308 mechanical CM	300	60	0.004	Vane
75 kHz TeleDyne RDI ADCP	30	1[a]	0.03	Central
75 kHz TeleDyne RDI ADCP	900	1[a]	0.02	Central
Nortek AquaDopp	5	1	0.01	One-side bar
Nortek AquaDopp	900	10	0.01	One-side bar
Aanderaa RCM11	900	12	0.005	Central

[a] Every acoustic ping.

Table 2
Different mooring characteristics. R denotes 75 kHz RDI-ADCP, N=Nortek AquaDopp, V=Valeport BFM-208 and A=Aanderaa RCM11.

Name	DOC09/2	DOC07/1	LOCO11/4	LOCO18/4
Latitude	01°24.5′N	00°44.2′N	30°00.0′N	02°30.2′N
Longitude	38°37.3′W	39°51.2′W	23°00.0′W	38°01.6′W
Water depth (m)	3263	1172	5140	4474
Startdate	23/06/09	05/12/07	23/11/07	11/12/07
Duration (days)	7	8	595	565
Cable dia. (m)	0.007	0.009	0.007	0.007 (Steel coated)
Cable length (m)	2550	295	3800	3450
Instruments	R	N	R	R, V, N, A
Sampl. period (s)	30	5	900	900 (N: 1 s for 30 s every day)
Typ. cur. sp. ($m\,s^{-1}$)	0.15	0.10	0.15	0.15
Max. cur. sp. ($m\,s^{-1}$)	0.30	0.30	0.25	0.25

and their potential effects on current observations. Values are related to observed rotations from Section 4.

Firstly, we assume a fast rotation of $5^\circ\,s^{-1}$ and a 1 s compass update. If the acoustic ping is not related to the compass update, the compass will maximally show and error of $\pm 2.5^\circ$, which is equivalent to typical compass accuracies, say instrumental noise. The effects on current measurements will be negligible, with perhaps some noise increase.

Secondly, we consider a compass update every 10 s. Slow rotation rates of up to $1^\circ\,s^{-1}$ will show similar negligible errors as

above. Fast rates of up to $10^\circ\,s^{-1}$ can show maximum mismatches of up to $\pm 50^\circ$, if the acoustic ping is not sampled simultaneously with the compass: for example when an instrument continuously sends out acoustic pings at the fastest rate possible and then silences during the remainder of an ensemble averaging period whilst slower rate compass updates are distributed over the entire ensemble period. Although not user-programmable, the contrary is done in e.g. Aanderaa RCM11's: a fixed number of pings (150) and, less, compass updates are evenly distributed over any, user-programmable, ensemble averaging period. This even distributing is recommendable, because if the compass update matches acoustic pings in time the current error due to a potential misreading of the compass will be much less than indicated above and it reduces to zero when a compass update and an acoustic ping are simultaneously sampled.

4. Observations

In a comparison study of linear open-ocean and non-linear near-bottom internal waves in the near-equatorial Ceará Basin (Brazil) we deployed two short-term moorings near a seamount: a bottom lander holding an acoustic current meter in its frame and one in a mooring line 150 m above the sloping bottom. Simultaneously, a long mooring line held two 75 kHz ADCPs, one looking upward, mounted in an elliptical buoy, the other looking downward, mounted in a rack. These two instruments were separated by a 1 m long chain and were located in 'open' waters, well above the top of the nearby seamount. The instrumentation sampled ensembles of acoustic pings relatively fast: every 5 s or faster on the bottom lander and every 30 s for the 75 kHz ADCPs. The latter's ensembles were averages of 8 pings, emitted at 1 Hz, but the instruments needed to be offset asynchronously by 15 s to avoid crosstalk.

The raw echo intensity data, I, of the 75 kHz ADCPs are dominated by the attenuation of sound away from them and by the regular diurnal pattern attributed to vertical plankton migration in several different groups or layers (Fig. 2a). Time is local solar and layers are clearly at their deepest point around noon. Some internal wave activity is visible as semidiurnal [tidal] or shorter period variations in the 'plankton layers', besides some high-frequency noise stretching across the entire vertical range and visible as blurs on the image, more clearly as detailed below.

This noise in acoustic echo seems to vary with a pattern that is neither semidiurnal nor diurnal. There is some, but not a unique association with the overall current amplitude, which is high due to spring tide in the beginning of the record and decreases towards neaps (Fig. 2b). This noise is strongly associated with sudden hefty variations in the heading of ADCPs (Fig. 2c). These heading variations are persistent for 1.5–5 h. As can be seen, the 'fast' spinning of instrumentation occurs or not; being either on or off, like a deterministic chaos bifurcal switch. For unknown reasons, spinning is only observed in the first half of the record just after spring tide, probably by chance. A similar exercise elsewhere demonstrated spinning throughout the one-week record. There seems a tendency of occurrence, although not exclusive, when the current speed at the depth of the ADCPs is relatively weak within the tidal period.

In more detail (Fig. 3), the change in echo-noise character is visible as an abrupt change from horizontal banding of highly variable reflectors (no spin) to an image blurred by very high frequency, vertically lines (spin on) (Fig. 3a). Henceforth, echo intensity is given relative to its time mean $\langle I\rangle(z)$ per depth level z, to remove acoustic attenuation through the water column. No noticeable variation in noise is observed in the current amplitude (Fig. 3b), and no noticeable variation is observed in current direction (not shown). However, the association with heading (Fig. 3c) and tilt (Fig. 3d) variations is very clear. The heading varies up to $180 \pm 20^\circ$ in a 30 s sampling period. Note that tilt never is more than 1.1°, confirming the near-upright mooring.

This is better visible in further detail (Fig. 4), where in panel c each individual data point is marked for the red graph. Its variations occur simultaneously in both ADCPs, accounting for the 15 s delay between them, and they are regularly under-sampled: this spinning is relatively fast over large angles, not just a swing. The physically coupled ADCPs allow precise study of the spin due to the asynchronously sampling despite the rather coarse sampling rate. When one is synchronized to the other by linear interpolation, the heading difference becomes identical during periods of spin on and no spin (Fig. 4c, purple stars). This is within

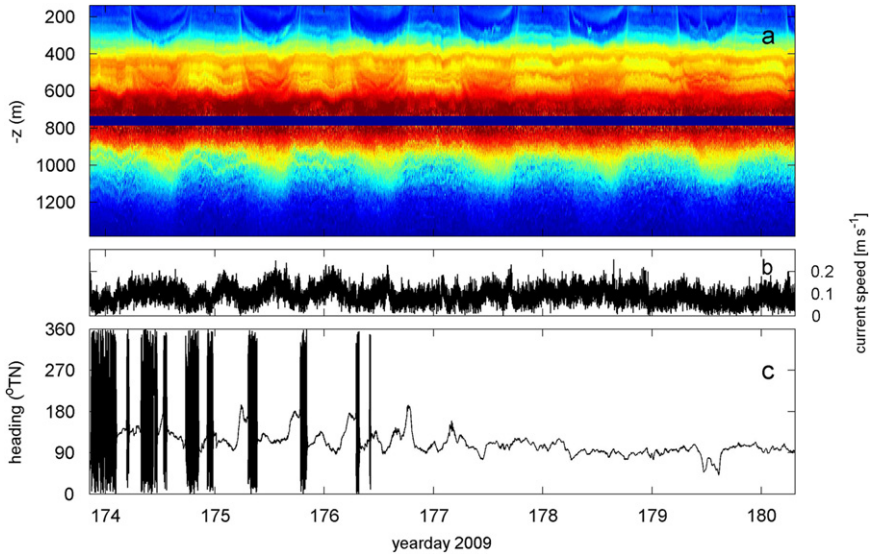

Fig. 2. (a) Time series of nearly one week of raw echo intensity from a double 75 kHz ADCP mooring DOC09/2 sampling at once per 30 s. Color scale between [20, 80] dB, blue-red. The band in the middle, around 800 m, is no or bad data due to the blanking distances above and below the upward looking and downward looking ADCPs, respectively. (b) Current speed at 635 m. (c) Heading of the upper ADCP. (For interpretation of the references to color in this figure legend, the reader is referred to the web version of this article.)

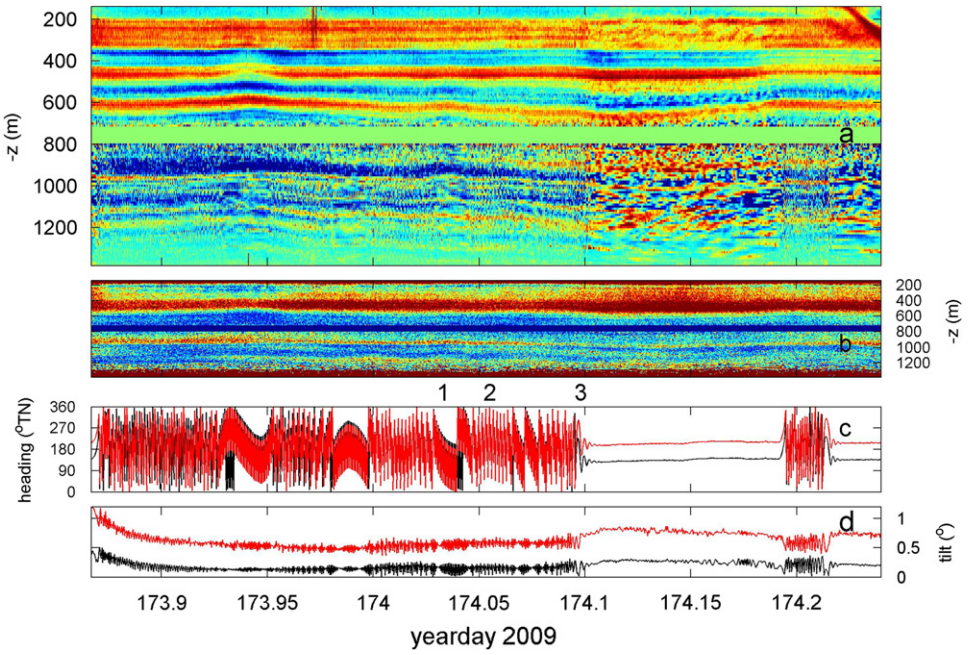

Fig. 3. Detail of observations in Fig. 2. (a) Echo intensity relative to time mean per depth level, color scale between [−6, 6] dB, blue-red. (b) Current amplitude, color scale between [0, 0.25] m s^{-1}, blue-red. (c) Heading of both ADCPs, in red for the lower one. The three numbered types of oscillations are described in the text. (d) As (c) but for tilt. The difference in mean tilt is solely due to unavoidable small errors in instrument mounting in frame and buoy. (For interpretation of the references to color in this figure legend, the reader is referred to the web version of this article.)

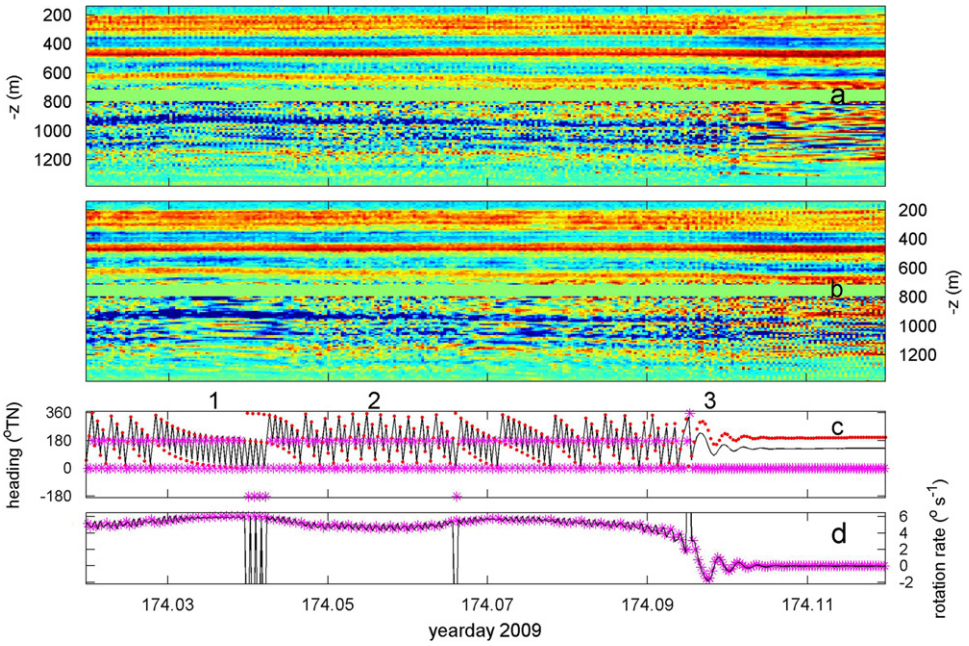

Fig. 4. Further detail of Figs. 2 and 3. (a) Relative echo intensity from beam 1. (b) As (a), but every other ensemble using the value of beam 2, the opposite to beam 1. (c) Heading, the red graph indicating each individual ensemble. Stars in purple indicate heading difference +70° (mean during no spin period) after synchronizing the red graph to the black via linear interpolation. (d) Rotation speed computed by first differencing the heading record (black) and by computing the heading difference of the asynchronously sampling instruments (purple stars).

a multiple of π due to wrap around and noise. It demonstrates the precise 'spot-on' sampling of the two independent flux-gate compasses, even under rotation speeds between 4.5 and $6.5 \pm 0.2^\circ\ s^{-1}$ (Fig. 4d).

These speeds can be accurately computed by either first-differencing the original heading signal (purple star) or by computing the heading difference between the ADCPs accounting for the 15 s time difference (black graph). Apart from a few wrap-around glitches, both methods show very nearly the same result. The second method also demonstrates the rotation sense of ADCPs, which remains the same (clockwise) during this particular example, so that the ADCP must make full rotations. This is concluded because the heading difference does not change sign, except during the last transitional period to no spin.

During spin on, three types of heading variations are reflected in three different types of high-frequency noise in relative echo intensity $dI(z)=I-\langle I\rangle$, through most of the vertical range $\Delta z > 1000$ m, thus being range-independent. There is no

particular sequence of occurrence between the types. Describing them in arbitrary order: One is a "regular" variation of about 180° between ensembles being an unresolved complete spin, with a slow modulation. This creates a regular noise pattern in dI, with values systematically higher or lower between neighbouring ensembles and little changes every other ensemble. As 180° heading change implies beam 1 occupying the position of beam 2 the next ensemble and vice versa, same for interchange of positions of opposing beams 3 and 4, the echo image of beam 1 in Fig. 4a was 'recomputed' with beam 2's dI_2 replacing dI_1 every other ensemble (time step). The result, Fig. 4b, shows no noise anymore during the regular heading variations like period '1' between days 174.03 and 174.04, and, of course, a regular apparent noise during a period with no spin (e.g., around day 174.11). An explanation is discussed in Section 5. The second heading variation varies slightly slower with time, covering the entire 360°-range through proper spin and generating irregular noise patterns in dI. A third is the "end-swing" of typically three damped oscillations, marking the end of a spin on period. Onset of a spin on period is always within a single slow period of about 2–3 min duration.

The typical spinning speed is $5^\circ\,s^{-1}$, which implies that the return ping is just outside the 1.5° main beam width of each ADCP for a total travel time of about 0.8 s for an acoustic ping. One would thus expect a range-dependent effect on the echo amplitude by a few dB at least, due to such misalignment. However, relative echo profiles during spin on and no spin do not show any significant differences to within an error of ± 1 dB (Fig. 5). Over the vertical range, the mean difference between such profiles amounts 0.1 dB. In contrast, the standard deviation of the noise varies from 1.3 ± 0.2 dB between adjacent profiles during no spin to 2.5 ± 0.3 dB during spin on. As noted before, this variation is range-independent compared to the log-linear variation of echo due to sound absorption and attenuation with distance from the instrument. Variations do occur, however, between the ADCPs as in general scatterers do become less with depth.

This variation in profiles is reflected in high-frequency noise variance levels at a particular depth. If we compare the noise levels of various ADCP-variables during spin on and no spin by selecting equally short periods of a couple of hours, we see that only the high-frequency noise levels of the echo intensity are significantly affected, indeed by about half a decade in variance (Fig. 6). The spectra of currents, horizontal and vertical, are not visibly affected in their flat white noise levels. This confirms the time series observations. Apparently, the averaging across the beam spread for current computations smooths the spin-effects below instrumental (acoustic) noise levels. In contrast, spin-effects dominate over acoustic noise for the in-beam echo intensity, perhaps in combination with varyingly distributed scatterers.

A similar conclusion is reached from a spectral analysis of currents measured using a non-vaned Nortek current meter mounted in-line, and moderately spinning, in comparison with data from a similar one mounted in a bottom-fixed frame for short-term observations at a slope near the top of a seamount (Fig. 7a). The heading of the latter instrument is indeed not significantly varying with time (Fig. 7b). The in-line instrument swings, but only across some 30–50° typically, without entire spin rotations. The effects in kinetic energy noise increase are only noticeable for frequencies $> 10^3$ cpd, cycles per day, and are hard to attribute to, still rapid, swinging per se, where they can be attributed to water turbulence as well.

Such turbulence is more vigorous at some vertical distance O(10 m) off the sloping bottom (Hosegood and van Haren, 2003). This is also reflected in the echo intensity with increases up to 30 dB above background level (van Haren, 2009), which is mostly dominated by resuspended sediments in turbulent flows. As a result, echo intensity is thus not useful for noise investigations due to mooring swing in this configuration. In this bottom lander & thermistor string mooring the cable tension is about 2000 N, about half that of the previously described mooring and perhaps not enough to start up large-scale spinning.

Large-scale rapid swing and spin are observed by the daily diagnosed AquaDopp's in about 3800 m long deep-ocean moorings for long-term observations. These moorings also have an average tension that is about twice the one in the bottom lander mooring. During 'spin on' periods the swing in the long-term mooring can be as fast as 7 s periodicity with angle amplitude of 20° (Fig. 8a). Such swings cannot be induced by surface waves, as the top of each mooring is never closer than 1000 m from the surface. They are also unlikely related to mooring vibrations, not swings, at the Strouhal frequency, which yield periods of about 0.2 s under typical governing currents for line-induced vibrations. However, for instrument vibrations the Strouhal period can reach about 5 s, which would explain the fastest swings if vibrations are transferred to rotations. Larger variations of 130–180°, say 'spin', have periods of 12 and 25 s, respectively, between half of and equal to that observed by the ADCPs in the mooring described above.

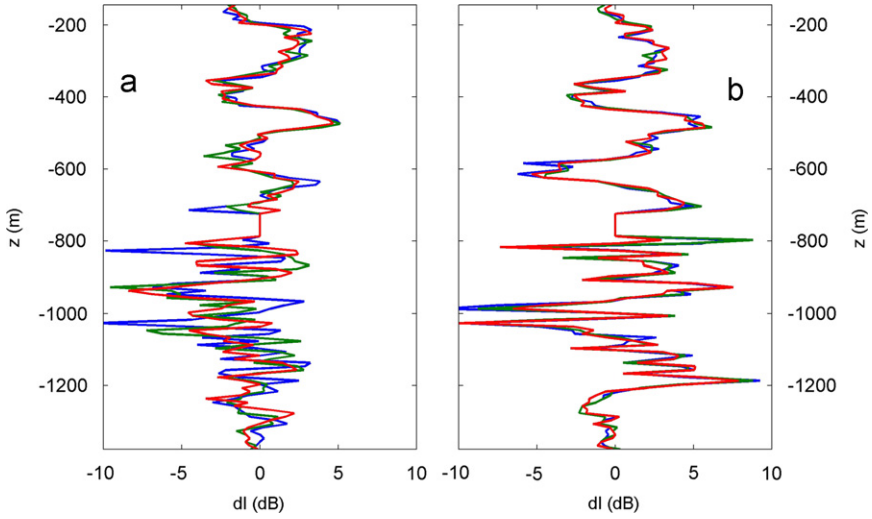

Fig. 5. Three consecutive profiles of relative echo intensity from Fig. 4 for two different periods. (a) Spin on, around day 174.06. (b) No spin, around day 174.12.

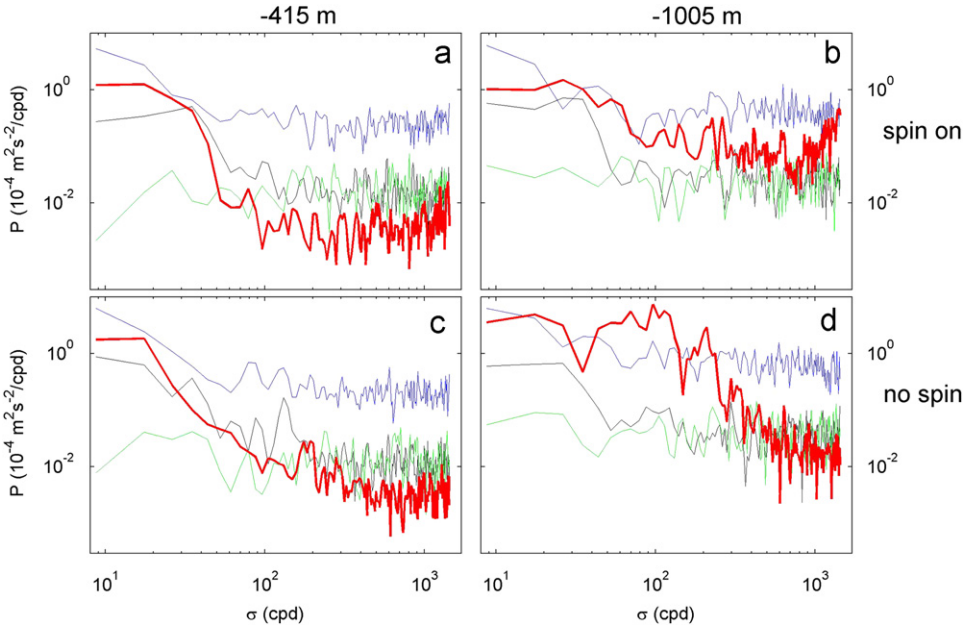

Fig. 6. Nearly raw spectra of 5 h portions of observations as in Fig. 2 of kinetic energy (blue), vertical current (black), error velocity (green), echo intensity (red; arbitrary units). (a) Upper ADCP, depth bin 28 during a period of spin on (173.87–174.10). (b) As (a), but for lower ADCP, bin 28. (c) As (a), but for period of no-spin [177.0–177.22]. (d) As (c), but for lower ADCP, bin 28. (For interpretation of the references to color in this figure legend, the reader is referred to the web version of this article.)

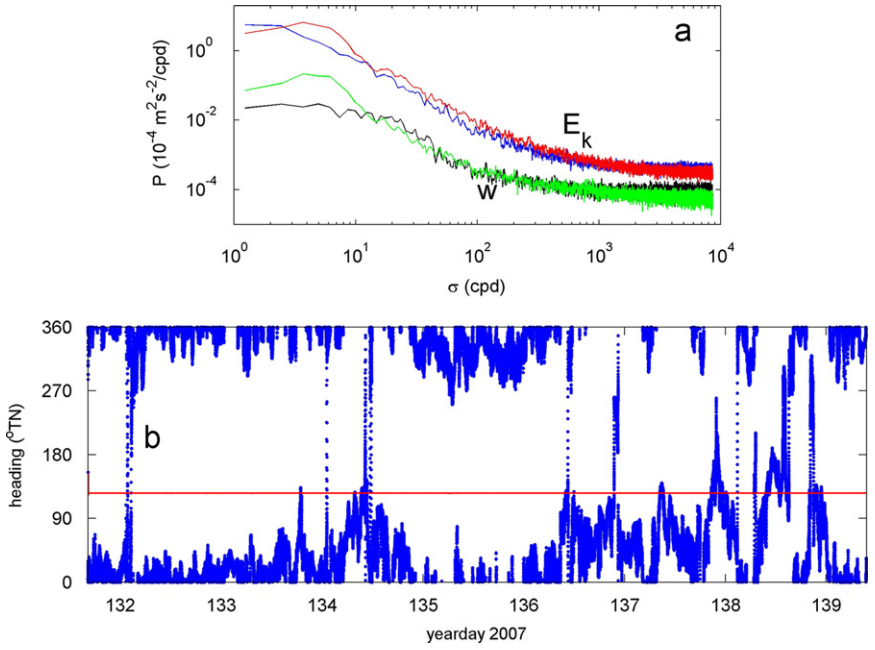

Fig. 7. AquaDopp observations sampled at once per 5 s for a period of one week at mooring DOC07/1, comparing a free-to-rotate inline instrument with a bottom-frame mounted instrument about 300 m below the former. (a) Spectra of the entire record for kinetic energy (blue, red) and vertical current variance (black, green; deliberately offset vertically) for inline and frame instruments, respectively. (b) Heading for inline (blue, dotted) and frame instruments (red, thin solid). (For interpretation of the references to color in this figure legend, the reader is referred to the web version of this article.)

Although the 30 s diagnostics were made only once per day, their statistics show that swinging occurs frequently through the entire 1.5 years record, with vehement spin occurring rarely (Fig. 8b). Standard deviation of heading variations has a mean of 11° and seldom exceeds 25°.

The overall effects of swing on kinetic energy levels are very low following comparison with levels from other instruments, notably a freely suspended and vaned Valeport mechanical current meter (Fig. 8c). Although we cannot rule out the existence of small swing on this vaned current device, Valeport's high-frequency noise levels are low commensurate the manufacturers estimate. These instruments are the only ones to allow resolution of the upper end of the internal wave band near the buoyancy frequency before rolling off. Harmonic semidiurnal and diurnal tidal motions have amplitudes to within 10% at all depths measured by different instruments, as expected for dominant barotropic motions. The variations in sloping noise levels in the internal wave band at frequencies between $1 < \sigma < 10$ cpd are partially attributable to different levels of internal wave energy, as scaled with varying buoyancy frequencies with depth, and

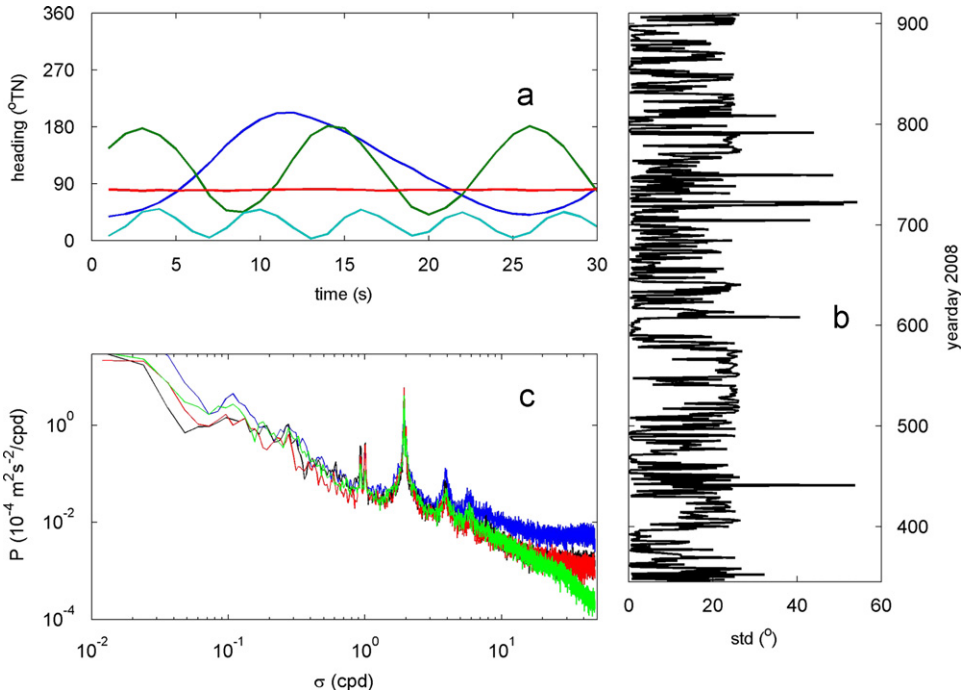

Fig. 8. One and a half years long measurements on mooring LOCO18/4. (a) Typical examples of 1 s sampled 'diagnostics' of AquaDopps' heading, run every day for 30 s. Three examples are for spin on, the red one is during no spin. Values are relative to arbitrary mean. (b) Standard deviation as a function of time of daily diagnostics of heading variations around their mean. (c) Kinetic energy spectrum of instrument in (a) (red), compared with those from 75 kHz ADCP (blue), Aanderaa RCM11 (black, scaled with buoyancy frequency) and Valeport mechanical current meter (green). (For interpretation of the references to color in this figure legend, the reader is referred to the web version of this article.)

partially due to acoustic noise and sampling volumes. The latter also dominates the different white noise levels for $\sigma > 10$ cpd, which are approaching noise levels indicated by the manufacturer being about 25 and 6 times the variance of the mechanical current meter for ADCP and AquaDopp, respectively.

5. Discussion

Acoustic current meters do not need a flow orientation with an asymmetric vane. Therefore, they can be more flexibly moored in a line. As a potential disadvantage, nearly symmetric devices under tension as in a taut-line mooring obstructing a flow have the tendency to swing or spin around their vertical axis. Potential errors in acoustic measurements may occur when the instrumentation read-out or update of compass or acoustic pings aliases the rotational motion.

The investigated instruments are all 'standard' devices designed to measure ocean currents, not turbulence. Ocean currents have typical periodicities O(10^2–10^6 s), but are resolved with acoustic ping updates at 1 Hz and compass updates at 0.1–1 Hz. The commonly used fast-response flux-gate compasses easily resolve such updates.

The lowest of these update rates matches the periodicity of the fastest swings observed, which amounts a few $^\circ\,s^{-1}$, over a range O(10°). The same rotational speed is observed for the longer duration spin. Nevertheless, noise comparison between data from instruments of different make show negligible effects on current measurements due to rotation. However, they do show effects on high-frequency echo amplitude variations in ADCPs. The reason for this discrepancy in effects is found in the particular manner of measuring by an ADCP, or any other acoustic current meter.

Echo amplitudes are measured directionless within individual beams, which may rotate around through non-uniform clouds of acoustic scatterers. The footprint of a 75 kHz ADCP is large, an acoustic beam 'traveling' at a speed of O(10 m s^{-1}) during rotation. The reason why the echo-noise character changes from horizontally to vertically striped upon rotation is related to the vertical shear of the environment. This is concluded from the periods of regular noise and 180°-heading variation every 30 s, or an interchanging of positions of opposite acoustic beams. As the noise is not log-linearly dependent with range it cannot be related to a mismatch of reception of the backscattered signal: it has to do with variations in acoustic reflections at particular depths. This could have been orientation of reflectors, most commonly thought of as zooplankton, with current [direction], but no such correspondence is found (Fig. 9a and b). Instead, a linear relationship is found between (absolute values of) relative echo amplitude and their differences between alternating ensembles, or positions of opposing beams (Fig. 9d). Furthermore, an inverse linear relationship is found between echo variations and vertical current shear (Fig. 9b and c): layers of large shear correspond to layers of weaker echo variations with time, and their difference between beam positions, and vice versa. As larger shear is supported by larger stratification, thereby suppressing turbulence, it presumably suppresses scatterers and their movements. This may explain the inverse relationship between shear and echo magnitudes, or a linear relationship between turbulence and scatterers and varying distribution. Alternatively, part of the observed echos are in fact turbulence, as has been suggested by (Ross and Lueck, 2003), so that the present echo amplitudes are more related with the state of high-frequency water motions than with zooplankton scatterers.

In contrast, ADCP's current measurements are averages over the beam spread. Currents are not measured in tangential direction but exclusively in longitudinal direction. As a result, firstly, instrument rotation of the beams does not introduce any error in the [beam-]current measurement, provided compass updates resolve the rotation. Secondly, the small change in positioning of the beam during a ping under rotation, which can

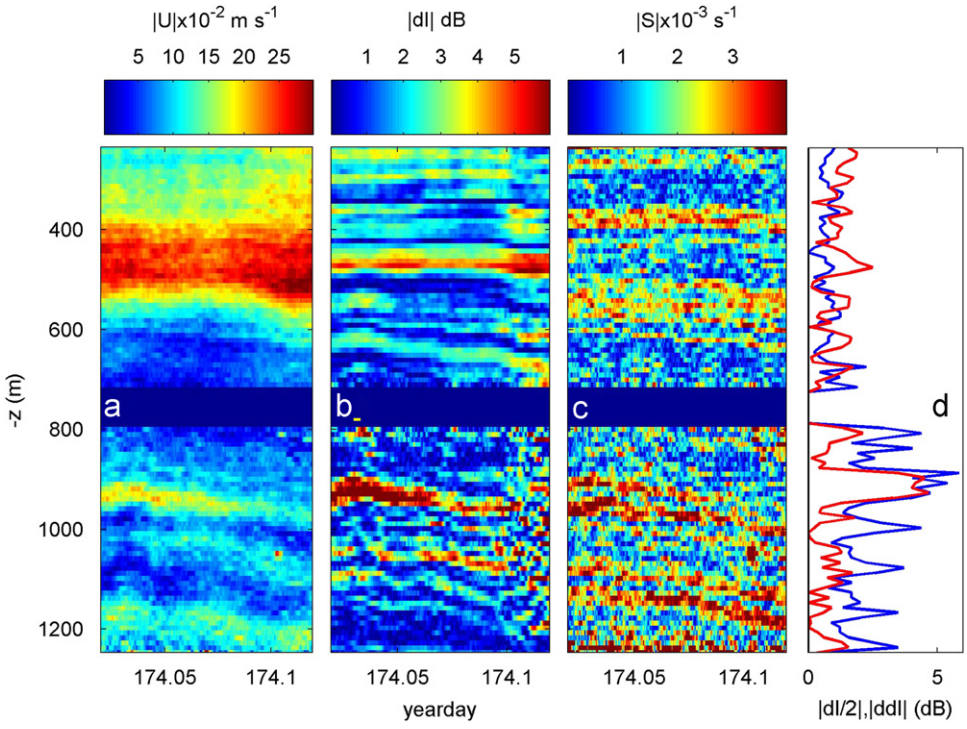

Fig. 9. Depth–time comparison of echo [noise] variations with current and shear for the period of Fig. 4. Data are smoothed using running mean over 10 points (300 s). (a) Current amplitude. (b) Absolute value of relative echo intensity for beam 1. Yellow dash under (b) indicates period of panel (d). (c) Current shear amplitude. (d) Averages over period 174.03–174.033 for absolute values of relative echo amplitude (/2; red) and average of absolute values of differences between echo amplitudes of consecutive ensembles (blue). (For interpretation of the references to color in this figure legend, the reader is referred to the web version of this article.)

affect momentum flux measurements to about 10% (van Haren et al., 1994), apparently introduces smaller current variations than natural small-scale motions or current inhomogeneities over the horizontal beam spread. Thirdly, compass updates are exactly matched with acoustic pings, and reasonably so for other instruments when possible. Fourthly, an ADCP shows much larger errors due to vertical and horizontal averaging, which for a 75 kHz system are typically 10 and 100 m, respectively, in combination with acoustic noise due to low amounts of scatterers in the open ocean. The footprints of single-point acoustic current meters are typically 1×5 m, vertical $\times$ horizontal, which comprises an order of magnitude larger volume than for a mechanical current meter, 0.5×1 m. This might explain the observed different roll-offs beyond the buoyancy frequency to turbulent scales.

The observed effects of swing and spin on ADCPs echo amplitude do not hamper studies on internal waves and studies on vertical migration by, e.g., zooplankton. The noise is manifest in a different frequency range. The negligible effects of swing and spin on current measurements are reassuring that the non-vaned mounting can be used safely. The use of vanes to acoustic instruments will not substantially improve their lesser performance in clear open ocean waters, specifically for internal wave studies, for which mechanical current meters behave better. This has probably little relationship with the signal-to-noise ratio of acoustic devices, which have been significantly improved recently (Hogg and Frye, 2007).

Acknowledgments

I thank the crew of the R/V Pelagia for deployment and recovery of moorings and Theo Hillebrand and NIOZ-MTM for their preparation. I thank Louis Gostiaux and anonymous reviewers for their remarks and suggestions. Instrumentation and deployment were financed in part by investment grants ('Oceanographic equipment' and 'LOCO', respectively) from Netherlands organisation for the advancement of scientific research, NWO. Some deployments were financed in part by BSIK.

References

Bagchi, P., Balachandar, S., 2002. Effect of free rotation on the motion of a solid sphere in linear shear flow at moderate Re. Phys. Fluids 14, 2719–2737.
Hogg, N.G., Frye, N.G., 2007. Performance of a new generation of acoustic current meters. J. Phys. Oceanogr. 37, 148–161.
Hosegood, P., van Haren, H., 2003. Ekman-induced turbulence over the continental slope in the Faeroe–Shetland channel as inferred from spikes in current meter observations. Deep-Sea Res. I 50, 657–680.
Loder, J.W., Hamilton, J.M., 1991. Degradation of some mechanical current meter measurements by high-frequency mooring or wave motion. IEEE J. Ocean. Eng. 16, 343–349.
Pollard, R., 1973. Interpretation of near-surface current meter observations. Deep-Sea Res. 20, 261–268.
Ross, T., Lueck, R., 2003. Sound scattering from oceanic turbulence. Geophys. Res. Lett. 30, 1344, doi:10.1029/2002GL016733.
Saunders, P.M., 1980. Overspeeding of a Savonius rotor. Deep-Sea Res. 27A, 755–759.
Schott, F., 1988. Effects of thermistor string mounted between the acoustic beams of an acoustic Doppler current profiler. J. Atmos. Ocean. Technol. 5, 154–159.
Sherwin, T.J., 1988. Measurements of current speed using an Aanderaa RCM4 current meter in the presence of surface waves. Cont. Shelf Res. 8, 131–144.
van Haren, H., 2009. Using high-sampling rate ADCP for observing vigorous processes above sloping [deep] ocean bottoms. J. Mar. Syst. 77, 418–427.
van Haren, H., Oakey, N., Garrett, C., 1994. Measurements of internal wave band eddy fluxes above a sloping bottom. J. Mar. Res. 52, 909–946.
von Zweck, O.H., Saunders, K.D., 1981. Contamination of current records by mooring motion. J. Geophys. Res. 86, 2071–2072.